Analysis of the solar wind IMF B_z and auroral electrojet index during supersubstorms

Drabindra Pandit[1,2], Narayan P. Chapagain[3], and Binod Adhikari[2,4]

Received 24 June 2020; accepted 17 May 2021; published 4 November 2021.

This work examines the coupling between solar wind interplanetary magnetic field (IMF B_z) and auroral electrojet (AE) index during supersubstorms (SSSs) of 11 April 2001 and 24 November 2001. The SSSs are particularly intense substorms with the value of $SML < -2500$ nT; $AL < -2500$ nT. For the detail analysis, the data set of 1 min time resolution of IMF B_z and AE index in the geocentric solar magnetospheric (GSM) coordinate system are used. The spectral characteristics of SSSs events are studied using continuous wavelet transforms (CWT) and global wavelet spectrum (GWS). The cross-correlation analysis also has been applied to study the correlation and time lag between IMF B_z and AE index. The spectrum identified the main periodicities of the IMF B_z and AE index during these events. The short-lived periodicity of high-frequency signals are identified between 70 to 256 minutes and 80 to 256 minutes during 11 April 2001 and 24 November 2001, respectively. The global wavelet spectrum (GWS) identifies the most energetic periods are present during the SSSs. Cross-correlation analysis shows that the AE index correlates (correlation coefficient ~ -0.6) with IMF B_z at time lag of approximately zero. These results support the previously existing facts that the magnetic reconnection between southward directed IMF B_z and the northward pointed Earth's magnetic field at the dayside magnetopause is the primary mechanism for transferring solar wind energy into magnetosphere and ionosphere during the SSSs events.
KEYWORDS: Geomagnetic index; interplanetary magnetic field; supersubstorms; magnetosphere; magnetic reconnection.

Citation: Pandit, Drabindra, Narayan P. Chapagain, and Binod Adhikari (2021), Analysis of the solar wind IMF B_z and auroral electrojet index during supersubstorms, *Russ. J. Earth. Sci., 21,* ES5006, doi:10.2205/2021ES000771.

1. Introduction

Magnetospheric substorm is one of the prevailing and elementary phenomena, occurs due to energy deposition into the Earth's magnetosphere and ionosphere [*Akasofu,* 1964]. The Substorm accompanied by a short-lived surge in earthward convection in the magnetotail followed by a global change in the magnetic morphology of the tail, representing a transfer of stored magnetic energy due to imbalance in the day-side and night-side reconnection rates [*McPherron et al.,* 1973]. During magnetic reconnection between southward directed IMF and the northward pointed Earth's magnetic field at the dayside magnetopause, energy is transferred into magnetosphere/magnetotail [*Tsurutani and Meng,* 1972; *Echer et al.,* 2008]. The substorms were believed as the integral part of the magnetic storms [*Gonzalez et al.,* 1994] but later it was found to occur independent of the storm

[1]Central Department of Physics, IOST, Tribhuvan University, Kirtipur, Kathmandu, Nepal
[2]Department of Physics, St. Xavier's College, Maitighar, Kathmandu, Nepal
[3]Department of Physics, Amrit Campus, Tribhuvan University, Kathmandu, Nepal
[4]Department of Physics, Patan Multiple Campus, Tribhuvan University, Lalitpur, Nepal

http://rjes.wdcb.ru/doi/2021ES000771-res.html

[*Tsurutani and Meng,* 1972] and also outside the main phase of the magnetic storm [*Hajra et al.,* 2013]. Supersubstorms (SSSs) are very intense substorms with large values of the SML or AL indices < -2500 nT [*Tsurutani et al.,* 2015]. The SML index is the generalization of the AL index, calculated by all stations of the SuperMAG network located not only at auroral latitude ($\sim 60^\circ$ to 70° geomagnetic latitudes) but also located at other higher and lower latitudes [*Gjerloev,* 2012; *Rostoker,* 1972].

The SSSs as an isolated event was invented by *Tsurutani et al.* [2015]. They pointed out that the SSSs are triggered by a small region of very high-density solar wind pressure pulse impinged upon the magnetosphere with a duration ranging from 17 to 50 minutes. The SSSs events are recorded by the long-term southward direction of IMF B_z. *Hajra et al.* [2016] found that SSSs occurred during all phases of the solar cycle, but the highest occurrence rate of 3.8 year^{-1} identified in descending phase, while the smallest frequency appeared during the minimum phase of the solar cycle. Their study also showed about 77% of SSSs related to a small region of very high-pressure pulses impinge upon the magnetosphere. It was shown by *Despirak et al.* [2018] that 42% of SSSs events were observed during the magnetic cloud (MC), 45.2% in the sheath, and 8.3% in the ejecta. *Despirak et al.* [2019] studied two supersubstorms that occurred during the strong magnetic storm on 7–8 September 2017 and found that ionospheric currents developed during SSSs were recorded on the global scale around the Earth. *Despirak et al.* [2021] in their recent paper entitled "Longitude geomagnetic effect of the SSSs during magnetic storm of March 9, 2012" mentioned that the effect of SSSs developed on a global scale in longitude, from before midnight, through the night and morning, and also into the day sector. *Henderson et al.* [1996] showed that periodic activity like sawtooth events found directly correlated with corresponding solar wind dynamic pressure enhancements. *Sergeev* [1996] suggested the energy flow from the solar wind into the magnetosphere becomes too large to dissipate without the periodic occurrence of substorms. Using CWT analysis, *de Souza et al.* [2018] analyzed the behavior of HILDCAAs event occurring between 1995 to 2011 and noted that the main periods of AE index lying between 4 and 12 h, which is 50% of the total identified periods. The paper by Srebrov et al. (Srebrov et al., 2019, Wavelet Analysis of Big Data in the Global Investigation of Magnetic Field Variations in Solar-Terrestrial Physics. arXiv preprint arXiv:1905.12923) reported that modes (wave packages) with different periods, the order of 20 to a few hundred minutes with a significant amplitude detected in the CWT analysis of a large amount of heterogeneous data of geomagnetic field, ionospheric parameters, and IMF. *Maggiolo et al.* [2017] analyzed the delay in time response of geomagnetic activity to the solar wind and obtained a good correlation between IMF B_z and AE with a correlation coefficient of -0.5. *Echer et al.* [2017] pointed out that the response of the IMF B_z during the September/October 2003 storm and noted that the main periodicities for the cross-correlation during 1.8 to 3.1 hours.

This paper aims to study the couplings between the IMF B_z and auroral electrojet index during two supersubstorms events. The events, data sets, and adopted methodologies are described in section 2. A brief description of the results and discussion are presented in section 3. Conclusions of the entire work are discussed in section 4.

2. Methodology

In this work, two supersubstorms events during 11 April 2001 and 24 November 2001 were selected using a threshold of SuperMAG $AL/SML < -2500$ nT as suggested by *Tsurutani et al.* [2015]. The data set for interplanetary parameters of 1 min time resolution were downloaded from the OMNI website https://omniweb.gsfc.nasa.gov/form/omni_min.html). The wavelet transforms, particularly continuous wavelet transforms (CWT) at different scales and the cross-correlation techniques (CCT) are used to find the relation between IMF B_z and AE index. The CWT is used to divide continuous time-series data into wavelets which use a very redundant and finely detailed description of a signal in terms of time and frequency. If a and b represent the dilation and translation parameters that vary continuously, then the continuous wavelet transform becomes

$$W(a,b) = \int f(t)\varphi^*\left(\frac{t-b}{a}\right)dt$$

where φ^* represents complex conjugate of φ and the function $W(a,b)$ represents the wavelets coefficients. For $a > 0$, variation of scale parameter

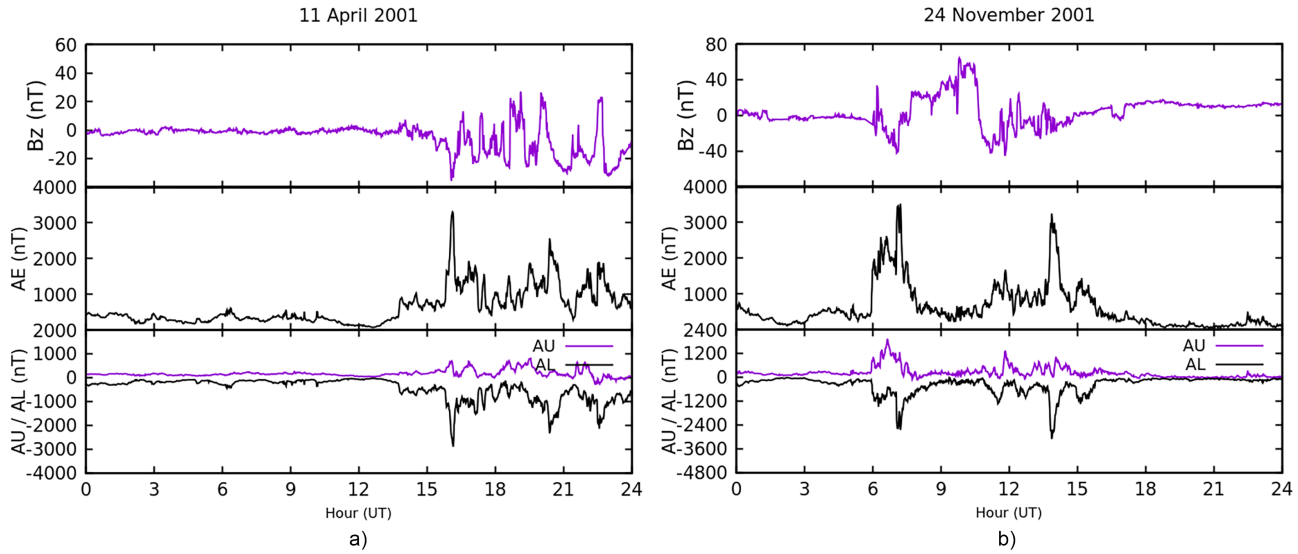

Figure 1. (a) and (b) from top to bottom represent: southward component of interplanetary magnetic field (B_z in nT), auroral electrojet index (AE in nT), auroral electrojet upper (AU in nT) and auroral electrojet lower (AL in nT) during two SSSs events occurred on 11 April 2001 and 24 November 2001, respectively.

gives dilation effect and for $a < 0$, it gives contraction effect of the mother wavelet function. It becomes convenient to identify the low and high frequency and longer and shorter duration present in the signal. For signal processing, a scalogram is used to visualize the wavelet transform which represents the square of the amplitude of the coefficient. It illustrates the distribution of signal energy in time, t, and scale a [*Adhikari et al.,* 2017a; *Lee and Yamamoto,* 1994]. The global wavelet spectrum (GWS) is also used to identify the most energetic periods present on the cross-wavelet analysis and it is obtained by

$$\text{GWS} = \int TW(a,b)|^2 db$$

The cross-correlation measures the similarity between variables in time series and also explores unseen information [*Adhikari and Chapagain,* 2015; *Liou et al.,* 2001]. The value of cross correlation lies near the vicinity of ± 1 implies the highest correlation and its value near zero showed moderate or low correlation [*Katz,* 1988]. The zero value of correlation infers no correlation between these two-time series variables. In this paper, cross-correlation is applied to obtain correlation coefficients and time lag between the IMF B_z and AE index.

3. Results and Discussion

In this section, we analyzed the solar wind IMF B_z and AE indices, and their coupling relationships using CWT, GWS, and cross-correlation analysis.

3.1. Solar Wind Interplanetary Magnetic Field (IMF B_z) and Auroral Electrojet Indices (AE, AU, AL)

Figure 1a and Figure 1b show an overview plot of the solar wind interplanetary magnetic field IMF B_z, auroral electrojet (AE), auroral electrojet upper (AU), and auroral electrojet lower (AL) indices associated with two SSSs events identified by the SML (AL) index < -2500 nT on 11 April 2001 and 24 November 2001, respectively. Two SSSs have occurred on each event day. On 11 April 2001, the day started as a quiet geomagnetic event with less fluctuation in IMF B_z represented at the top panel of the plot. There was southward turning of IMF $B_z \sim -39$ nT before the onset of the first SSS $\sim$15:20 UT. After the first SSS, a strong oscillation occurs in IMF B_z between 28 nT to -25 nT and it becomes several times negative around peak value -25 nT, caused by the Alfven waves [*Guo et al.,* 2016]. This is a common feature of a solar wind

stream associated with a coronal hole. A strong energy coupling and modulation of the magnetosphere by an intermittent but strong southward component of IMF B_z are favorable for the development of aurora [*Echer et al.,* 2017]. The second panel shows the variation of the auroral electrojet index which acquired peak values 3500 nT and 2500 nT during the first and second SSS events, respectively. A higher *AE* index indicates enormous energy, which is indulged into the Earth's magnetosphere by transfer of energy and momentum from the solar wind. Consequently, high Joule heating is produced near high latitude. During Joule heating, particle flux precipitated collides with neutral gas and loses its kinetic energy near the auroral region [*Suji and Prince,* 2018]. The third panel of Figure 1a reproduces the *AU* and *AL* indices associated with SSSs. The first SSS event took place approximately from 15:53 UT to 16:33 UT for 40 minutes and the second SSS started after 4 hrs and 23 min gap approximately from 20:16 UT to 20:51 for 35 min as indicated by a sharp decrease in *AL* index. During the first SSS, the peak value of the *AL* index is −2903 nT around ∼ 16 : 09 UT and during the second SSS, the peak value of the AL index is −2339 nT around ∼ 20:23 UT. Similarly, the values of the *AU* index are 500 nT and 200 nT during the first and second SSSs, respectively. In general, the *AL* index takes highly negative value but with the mixing of magnetospheric ring current in ionosphere sometimes it may create small positive variation [*Adhikari and Chapagain,* 2015]. The maximum perturbation generated in the *AU* index gives strength of eastward electrojet and in the *AL* index; it gives the individual strength of westward electrojet [*Weimer et al.,* 1990].

Figure 1b is rather similar to the first but it shows the event of SSS of 24 November 2001. On the first panel of Figure 1b, the IMF B_z has a southward component of ∼ −28 nT and −21 nT prior to both SSS events. The southward component of IMF B_z is means of identifying solar energy transfer to magnetosphere through magnetic reconnection at the dayside magnetosphere [*Echer et al.,* 2008; *Hajra et al.,* 2016]. The *AE* index on the second panel ranging from 0 to 4000 nT, depicts two different SSS events that have occurred during the interval of 8 hr with the similar type of the highest peaks 3500 nT and 3200 nT. The two SSSs of 24 November 2001 occurred ∼ 07 : 00 UT and ∼13:45 UT for the duration of 50 min and 30 min, respectively. The peak values of the *AL* index found during two SSSs are −2500 nT and −3400 nT. Strong burst is not noticed in the *AU* index as the *AE* and *AL* indices. The value of the *AU* index was found to be ∼ 1200 nT and 600 nT during two SSSs events, respectively. The first SSS event was caused by southward IMF B_z in the sheath and the second event by southward IMF B_z in the magnetic cloud [*Tsurutani et al.,* 2015]. The two SSS events appear to be caused by interplanetary sheath [*Hajra et al.,* 2016] which is characterized by multiple IMF B_z changes.

Moreover, SSS is an isolated event; it can exit inside the superstorms, triggered by solar wind high-pressure pulse. This was noted by *Tsurutani et al.* [2015]. Seventy-four SSSs occurred within the year 1981 to 2012 were identified by *Hajra et al.* [2016]. Their study reported that SSSs can occur in all phases of the solar cycle with the highest occurrence frequency recorded in descending phase. They also show SSSs follow an annual variation. Their study again pointed out that 77% of SSSs were associated with a small region of very high increase in pressure pulses impinging upon the magnetosphere. [*Adhikari and Chapagain,* 2015] found that during SSSs the polar cap potential and merging electric field was a hundred times higher than it developed during high intensity long duration auroral activities (HILDCAAs). Variation of field-aligned current (FAC) along with solar wind parameters for three SSSs was studied by *Adhikari et al.* [2017b] and concluded that FAC is the prime cause for east-west perturbation of magnetic field at high latitude for SSS events to occur, during that instant the value of *AE* was found greater than 3000 nT. The study of ionospheric current by *Despirak et al.* [2019] during two SSS of 7–8 September 2017 found that the SSS has a global effect to the ionospheric current. The impact related to SSS was studied by *Tsurutani et al.* [2020] and pointed out that SSS events may occur within magnetic storms that can cause GIC due to strong dB/dt effect in-ground stations but by earlier researcher have been attributed to "magnetic storms" as the real cause of it. The increase in solar wind IMF B_z and auroral electrojet indices reveal the transfer of energy and momentum from the solar wind to the magnetosphere to produce the power outages on the Earth [*Tsurutani et al.,* 2015].

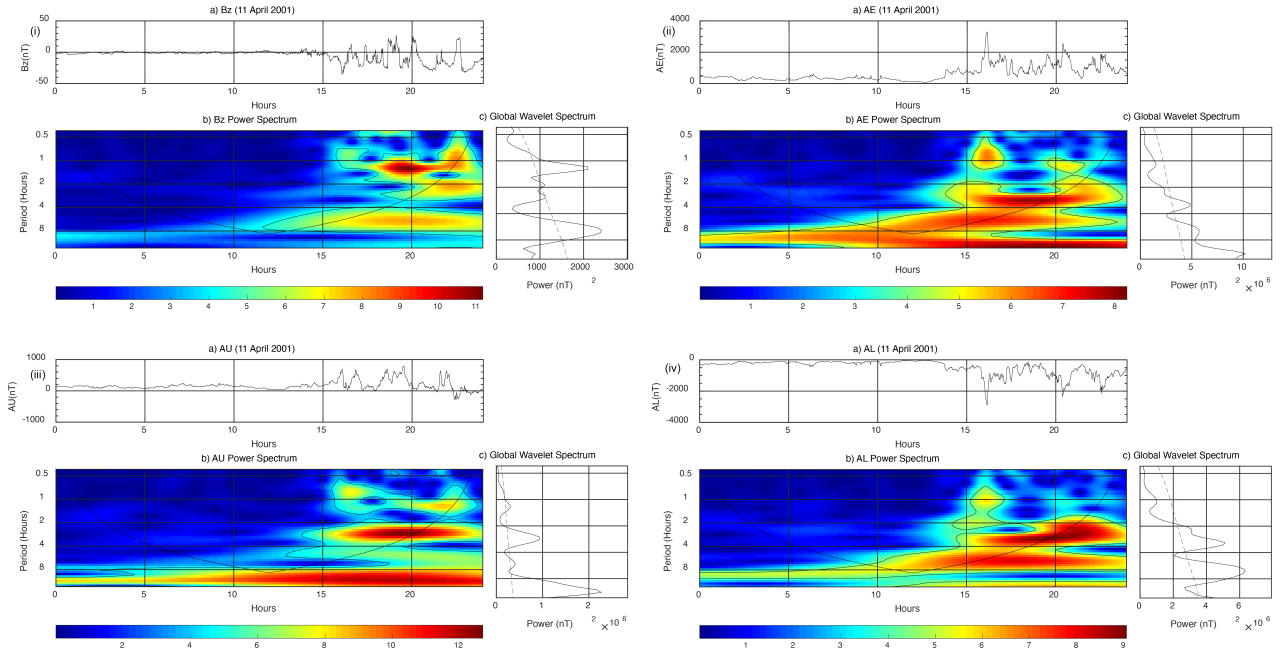

Figure 2. In (i) panel a) Time series of IMFBz b) Cross-wavelet spectrum periodogram during SSS of 11 April 2001 and c) The global wavelet spectrum shows the period of correlation. The (ii), (iii) and (iv) panel represent the same for AE, AU and AL, respectively.

3.2. Continuous Wavelet Signature

In Figure 2, the panel (i)–(iv) show a) the time series variations b) the power spectrum and c) the GWS of southward component of interplanetary magnetic field (IMF B_z), auroral electrojet index (AE), auroral electrojet upper (AU) and auroral electrojet lower (AL) during SSS on 11 April 2001, respectively. In the power spectrum plot, the square modulus of the wavelet coefficient provides the energy distribution in the time scale. A small perturbation in signal energy is visualized using a log2 function in wavelet space represented in the scalogram. It helps to understand the behavior of energy at a certain scale [*Domingues et al.*, 2005]. The abrupt change in the parameters such as magnetic field is characterized by a scalogram. These perturbations appear on scalograms through scattering frequencies even short and medium periods have their high amplitudes. The most important advantage of using scalogram analysis is to observe the distribution of amplitudes in larger scales. The horizontal axis in this figure represents time in an hour and the vertical axis represents the periodicity in minutes. The square of the actual amplitude of the wavelet coefficients represented in plots is indicated by the color bar on the right-hand side of the plot and has units in $(\mathrm{nT})^2$. They represent the square estimation of the actual value of the parameters. In the scalogram, the region of stronger wavelet power is shown in black (horizontal color indicator chart) and the region of low wavelet power is visualized in blue. The maximum and minimum wavelet power on the scalogram corresponds to high and low peak intensity. In each plot, it reveals highly variable signals in time without continuous periodicity. In Figure 2, the background intensity 1 $(\mathrm{nT})^2$ has found increased to 11 $(\mathrm{nT})^2$ for IMF B_z, 1 to 8 $(\mathrm{nT})^2$ for AE, 2 to 12 $(\mathrm{nT})^2$ for AU and 1 to 9 $(\mathrm{nT})^2$ for AL. The power area of higher intensity is seen time scale between approximately 2 to 1 and 5 to 4; AE between 16 to 4 and 4 to 2; AU between 16 to 8 and 4 to 2 and AL between 8 to 4 and 4 to 2 for time $\sim$ 16:00 UT and $\sim$ 20:00 UT, respectively for SSSs event of 11 April 2001, respectively. The results from the scalogram pointed out that some characteristics of solar wind and interplanetary parameters are confirmed the abrupt change in the magnetic field. The high intensity with max-

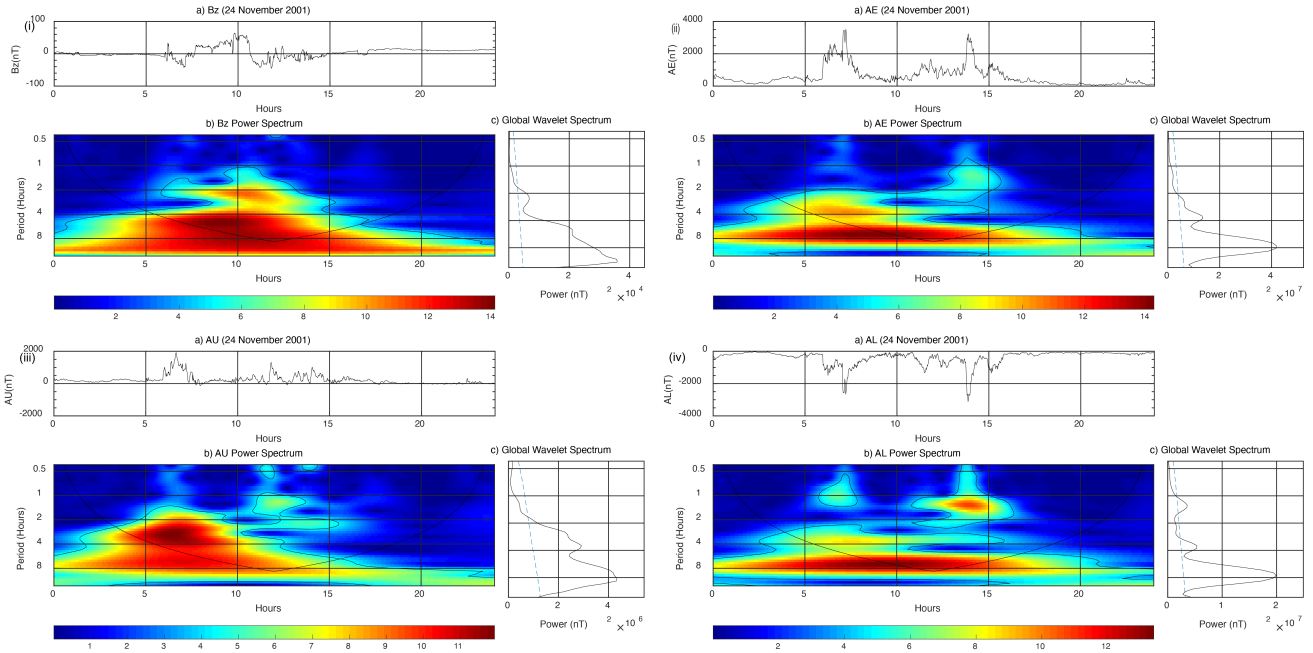

Figure 3. In (i) panel a) Time series of IMF B_z b) Cross-wavelet spectrum periodogram during SSS of 24 November 2001 and c) the global wavelet spectrum shows the period of correlation. The (ii), (iii) and (iv) panel represent the same for AE, AU and AL, respectively.

imum periodicity observed in all panels indicates the effect presented by the SSS events. The short duration trend has a significant effect on the indices AE, AL, AU, and IMF B_z during SSSs. It means that during the short pulse, thermal energy and energetic particles are injected into the magnetosphere/magnetotail which may cause a power blackout on the Earth.

Figure 3 is similar to Figure 2 but refers to the supersubstorm of 24 November 2001 in which two SSSs noticed the first SSS at ∼07:00 UT and the second at 13:45 UT. The small perturbation in signal energy is visualized using a log2 function in wavelet space represented in the scalogram. The scalograms for each parameter on 24 November 2001 follow the same numerical method as the previous event and its interpretation is the same as in the previous event. In Figure 3, the background intensity 2 $(\mathrm{nT})^2$ has been found increased to 14 $(\mathrm{nT})^2$ for the IMF B_z, AE, AL, and 1 to 12 $(\mathrm{nT})^2$ for AU indices, respectively. In Figure 3, the areas corresponding to strong power found for the IMF B_z between 16 to 4 and 4 to 2; AE between 10 to 6 and 4 to 2; AU between 8 to 4 and 4 to 2 and between 10 to 6 and 2 to 1 for time ∼07:00 UT and ∼13:00 UT of SSSs event of 24 November 2001, respectively. In each figure, some of the strong power areas lie outside the cone of influence. The IMF B_z, AE, AU, and AL indices have more or less the same spectral behaviors. Hence, there exists a one-to-one correspondence between the IMF B_z and the AE, AU, and AL indices. This wavelet analysis clearly supports the existing coupling between solar-wind-magnetosphere during SSS events. From this analysis, it can be understood that some characteristics effects are seen on auroral electrojet indices during the SSSs. These indices were highly disturbed at the time of SSSs, and the highest values of relative amplitudes are seen on scalogram. These relative amplitudes allow for the identification of quiescent and non-quiescent periods in the magnetic signals. Thus, using this tool, the intrinsic processes of energy transfer are being surveyed. This fact confirms the known concept that the penetration of charged particles and energy injection are more frequent during reconnection mechanism between the IMF B_z and geomagnetic field at magnetosphere during SSSs [*Mendes et al.*, 2004; *Morioka et al.*, 2003].

3.3. Global Wavelet Spectrum

The subplots (c) of Figure 2 and Figure 3 show the GWS of the IMF B_z, AE, AU, and AL indices during SSS on 11 April 2001 and 24 November 2001, respectively. It analyzes the distribution of the correlated major periods between the two variables. In Figure 2, the two periods of higher correlation be noticed at ∼16:00 UT and ∼20:00 UT with energy value 1500 and 2200 $(\mathrm{nT})^2$ for IMF B_z; 10×10^6 and 5×10^6 $(\mathrm{nT})^2$ for AE; 2.4×10^6 and 1×10^6 $(\mathrm{nT})^2$ for AU and 6×10^6 and 5×10^6 $(\mathrm{nT})^2$ for AL, which correspond with the duration of the two SSS occurred on 11 April 2001. In Figure 3, the two periods of higher correlation identified at ∼ 07:00 UT and ∼ 13:00 UT with energy value 3×10^4 and 2×10^4 $(\mathrm{nT})^2$ for IMF B_z; 4.2×10^7 and 1.5×10^7 $(\mathrm{nT})^2$ for AE; 4.2×10^6 and 3×10^6 $(\mathrm{nT})^2$ for AU; 2×10^7 and 0.5×10^7 $(\mathrm{nT})^2$ for AL during two SSS events of 24 November 2001. The paper by *Adhikari et al.* [2018] reported that the ICME related storm during 20–21 November 2003 correlation identified during the period of 64 to 16 with energy value 2.5×10^{10} V^2, HSS related storm of 17 July 2004 correlation identified during the period of 64 min with energy value 9×10^{10} V^2, ICME related substorm of 24 October 2002 correlation identified during period of 24 min with energy value 7.2×10^9 V^2. During study of SSS on 21 January 2005 *Adhikari et al.* [2018] found the correlation coefficient during the period of 30 min with energy value 9×10^{11} V^2 in Polar cap voltage (PCV). The IMF B_z, AE, AU, and AL indices have almost the same spectral characteristics and hence there is a one-to-one correspondence between the IMF B_z and AE, AU, and AL indices on both SSSs. These results support the existing correlation between the IMF B_z and AE, AU, and AL indices. Three periods of higher correlation were identified by *de Souza et al.* [2018] during the study of HILDCA with maximum energy 1.2×10^6 $(\mathrm{nT})^2$ due to efficient solar wind coupling between IMF B_z associates with Alfvan wave fluctuation and geomagnetic field which was identified as the main cause of geomagnetic activity related to HILDCA [*Tsurutani and Gonzalez,* 1987]. During SSS the short pulsation coupling mechanism between IMF B_z and geomagnetic field may cause large energy released for the destruction of space and terrestrial assets [*Tsurutani et al.,* 2015].

3.4. Cross Correlation Analysis

Figure 4a and Figure 4b represent the cross-correlation between the IMF B_z and AE index during two SSSs occurred at 15:53 UT and 20:16 UT on 11 April 2001 and Figure 4c and Figure 4d represent during two SSSs occurred at 07:00 UT and 13:45 UT on 24 November 2001. The cross-correlation determines the degree of correlation and time lag between two time series. In the plot, the horizontal axis represents time lags between two-time series and the vertical axis represents the correlation coefficient. The time scale in minutes indicates which index leads or lags before and after they get correlated. From Figure 4a–Figure 4d, it seems that IMF B_z and AE index correlated with a correlation coefficient ~ -0.6 approximately with zero-time lag. It can be interpreted as the prompt response on the AE index to the changes that occur on the IMF B_z. The prompt response in the AE index due to the perturbation of the IMF B_z during intense geomagnetic storm reported by *Pandit et al.* [2018] and they found the correlation between them with a coefficient 0.5. In *Adhikari et al.* [2018] observed correlation coefficient between FAC-AE is 0.8 with time lead of 50 min during SSS on 21 January 2001 and they also showed cross correlation between FAC-B_z in phase with correlation coefficient -0.5 at time lag of 60 min. The correlation between solar wind parameters and auroral electrojet lower (AL) index was studied by *Bargatze et al.* [1985] and found that two pulse peak responses in a time lag of 20 min for strong geomagnetic level and 60 min for moderate geomagnetic level. The first peak was associated with magnetospheric activity driven by solar wind coupling and the second was related to magnetospheric activity driven by the release of energy previously stored in the magnetotail. A study of SSSs of 20 November 2003 by *Poudel et al.* [2019] pointed out that the magnetospheric response to the solar wind invasion is pretty quick during the SSSs events and also showed a correlation coefficient between the IMF B_z and energy dissipated at auroral region (Ur) of -0.744 at zero-time lag. In this study, the correlation between the IMF B_z and AE was identified as high almost with no lag due to strong geomagnetic and auroral activities during magnetic reconnection between the interplanetary magnetic field and a north-south component of the geomagnetic field.

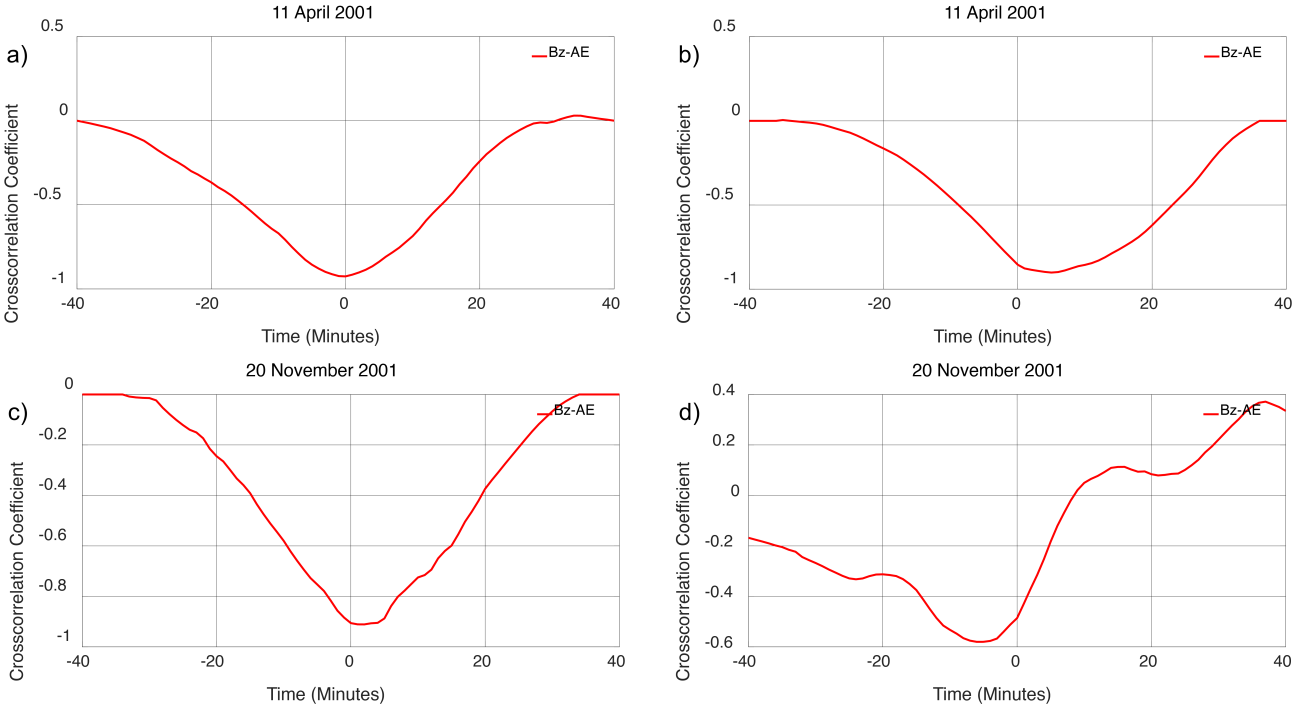

Figure 4. (a) and (b) Cross correlation between IMF B_z and AE index during two SSSs events occurred at 15:53 UT and 20:16 UT on 11 April 2001 and (c) and (d) represent the same during two SSSs events occurred at 07:00 UT and 13:45 UT on 24 November 2001.

4. Conclusion

In this work, we studied the solar wind-magnetosphere coupling during two supersubstorms (SSSs) events on 11 April 2001 and 24 November 2001. The time response of auroral electrojet index to solar wind interplanetary magnetic field (IMF B_z) during coupling has been analyzed using continuous wavelet transforms (CWT) and global wavelet spectrum (GWS) methods. The spectrum identified the main periodicities of the IMF B_z and AE index during these events. The short-lived periodicity of high-frequency signals are identified between 70 to 256 minutes and 80 to 256 minutes during 11 April 2001 and 24 November 2001, respectively. The global wavelet spectrum (GWS) identifies the most energetic periods are present during the SSSs. We also applied cross-correlation analysis to study the correlation and time lag between the IMF B_z and AE index. Through the correlation analysis technique, the correlation coefficient ~ -0.6 was obtained between the AE and IMF B_z approximately with zero lag. This study supports the previous existing facts that the solar wind-magnetosphere coupling during SSSs is mainly due to magnetic reconnection between southward IMF B_z and geomagnetic field at the magnetosphere.

Acknowledgments. We acknowledge Omni data site (https://omniweb.gsfc.nasa.gov/form/omni_min.html) for providing interplanetary magnetic indices data for our study. The author would like to acknowledge Nepal Academy of Science and Technology (NAST), Nepal for proving PhD fellowship to carry out this research project.

References

Adhikari, B., N. P. Chapagain (2015), Polar cap potential and merging electric field during high intensity long duration continuous auroral activity, *J. Nepal Phys. Soc.*, *3,* No. 1, 6–17, **Crossref**

Adhikari, B., P. Baruwal, N. P. Chapagain (2017a), Analysis of super substorm events with reference to polar cap potential and polar cap index, *Earth and Space Science*, *4,* 2–15, **Crossref**

Adhikari, B., S. Dahal, N. P. Chapagain (2017b), Study of field aligned current (FAC), interplanetary electric field component (E_y), interplanetary magnetic field component (B_z), and northward (x) and eastward (y) components of geomagnetic field during super substorm, *Earth and Space Science*, *4,* 257–274, Crossref

Adhikari, B., S. Dahal, et al(2018), Field-aligned current and polar cap potential and geomagnetic disturbances: A review of cross-correlation analysis, *Earth and Space Science*, *5,* 440–455, Crossref

Akasofu, S. I. (1964), The development of the auroral substorm, *Planet. Space Sci.*, *12,* 273–282, Crossref

Bargatze, L. F., D. N. Baker, et al. (1985), Magnetospheric impulse response for many levels of geomagnetic activity, *J. Geophys. Res.*, *90,* 6387–6394, Crossref

de Souza, A., M. E. Echer, et al. (2018), Cross-correlation and cross-wavelet analyses of the solar wind IMF B_z and auroral electrojet index *AE* coupling during HILDCAAs, *Ann. Geophys.*, *36,* 205–211, Crossref

Despirak, I. V., A. A. Lyubchich, N. G. Kleimenova (2018), Large scale structure of solar wind and appearance of supersubstorm, Physics of auroral phenomena, *Proc. XLI Annual seminar* p. 11–13, PGI, Apatity.

Despirak, I., N. Kleimenova, et al. (2019), Super substorms during strong magnetic storm on 7 September 2017, *E3S Web of Conferences*, *127,* 01010, Crossref

Despirak, I. V., A. A. Lyubchich, et al. (2021), Longitude Geomagnetic Effects of the Supersubstorms during the Magnetic Storm of March 9, 2012, *Bulletin of the Russian Academy of Sciences: Physics*, *85,* No. 3, 246–251, Crossref

Domingues, M. O., O. Mendes, A. M. da Costa (2005), Wavelet techniques in atmospheric sciences, *Advances in Space Research*, *35,* No. 5, 831–842, Crossref

Echer, E., W. D. Gonzalez, et al. (2008), Interplanetary conditions causing intense geomagnetic storms ($Dst \leq 100$ nT) during solar cycle 23 (1996–2006), *J. Geophys. Res.*, *113,* A05221, Crossref

Echer, E., A. Korth, et al. (2017), Global geomagnetic responses to the IMF B_z fluctuations during the September/October 2003 high-speed stream intervals, *Ann. Geophys.*, *35,* 853–868, Crossref

Gjerloev, J. W. (2012), The SuperMAG data processing technique, *J. Geophys. Res.*, *117,* A09213, Crossref

Gonzalez, W. D., J. A. Joselyn, et al. (1994), What is a geomagnetic storm qm?, *Journal of Geophysical Research*, *99,* 5771–5792, Crossref

Guo, J., F. Wei, et al. (2016), Alfvén waves as a solar-interplanetary driver of the thermospheric disturbances, *Sci. Rep.*, *6,* 18,895, Crossref

Hajra, R., B. T. Tsurutani, et al. (2016), Supersubstorms ($SML < 2500$ nT): Magnetic storm and solar cycle dependences, *J. Geophys. Res. Space Physics*, *121,* 7805–7816, Crossref

Hajra, R., B. T. Tsurutani, et al. (2013), Solar cycle dependence of high intensity long-duration continuous *AE* activity (HILDCAA) events, relativistic electron predictors?, *J. Geophys. Res. Space Physics*, *118,* 5626–5638, Crossref

Henderson, M. G., J. S. Murphree, J. M. Weygand (1996), Observationsof auroral substorms occurring together with preexisting "quiet time" auroral patterns, *J. Geophys. Res.*, *101,* 24,621–24,640, Crossref

Katz, R. W. (1988), Use of cross correlations in the search for teleconnections, *J. Climatology*, *8,* 241–253, Crossref

Lee, D. T. L., A. Yamamoto (1994), Wavelet analysis: theory and applications, *Hewlett-Packard Journal*, *45,* No. 6, 44.

Liou, K., P. T. Newell, C. L. Meng (2001), Seasonal effect on auroral particle acceleration and precipitation, *Journal of Geophysical Research*, *106,* 551, Crossref

Maggiolo, R., M. Hamrin, et al. (2017), The delayed timeresponse of geomagnetic activity to thesolar wind, *Journal of Geophysical Research: Space Physics*, *122,* 11,109–11,127, Crossref

McPherron, R. L., C. T. Russell, M. P. Aubry (1973), Satellite studies of magnetospheric substorms on August 15, 1968. Phenomenological model for substorms, *J. Geophys. Res.*, *78,* 3131–3149, Crossref

Mendes, O. J., M. O. Domingues, et al. (2004), Wavelet analysis applied to magnetograms: singularity detections related to geomagnetic storms, *VI Latin-American Conference on Space Geophysics* 1, p. 177, InstitutoNatcional de PesquisasEspaciais, Sao Jose dos Campos.

Morioka, A., Y. Miyoshi, et al. (2003), AKR disappearance during magnetic storms, *Journal of Geophysical Research*, *108,* No. A6, 1226–1235, Crossref

Pandit, D., N. P. Chapagain, et al. (2018), Activities and Its Impact on SpaceWeather, Long-Term Datasets for the Understandingof Solar and Stellar Magnetic Cycles Proceedings IAU Symposium No. 340, 2018 International Astronomical Union 2018, *Journal of Geophysical Research*, Crossref

Poudel, P., S. Simkhada, et al. (2019), Variation of solar wind parameters along with the understanding of energydynamics within the magnetospheric system during geomagnetic disturbances, *Earth and Space Science*, *6,* 276–293, Crossref

Rostoker, G. (1972), Geomagnetic indices, *Rev. Geophys.*, *10,* 935–950, Crossref

Sergeev, V. A. (1996), Energetic particles as tracers of magnetospheric configuration, *Adv. Space Res.*, *18,* 161–170, Crossref

Suji, K. J., P. R. Prince (2018), Global and local Joule heating during substorms in St. Patrick's Day 2015 geomagnetic storm, *Earth Planets Space*, *70,* 167, Crossref

Tsurutani, B. T., W. D. Gonzalez (1987), The cause of high-intensity long duration continuous *AE* activity (HILDCAAS): interplanetary alfven wave trains, *Planetary and Space Science*, *35,* 400–412, **Crossref**

Tsurutani, B. T., C. I. Meng (1972), Interplanetary magnetic-field variations and substorm activity, *J. Geophys. Res.*, *77,* 2964–2970, **Crossref**

Tsurutani, B. T., R. Hajra, et al. (2015), Extremely intense ($SML \leq 2500$ nT) substorms: Isolated events that are externally triggered?, *Ann. Geophys. Commun.*, *33,* 519–524, **Crossref**

Tsurutani, B. T., G. S. Lakhin, R. Hajra (2020), The physics of space weather/solar-terrestrial physics (STP): what we know now and what the current and future challenges are, *Nonlin. Processes Geophys.*, *27,* 75–119, **Crossref**

Weimer, D. R., L. A. Reinleitner, et al. (1990), Saturation of the auroral electrojet current and the polar cap potential, *Journal of Geophysical Research*, *95,* 18,981–18,987, **Crossref**

Corresponding author:
Drabindra Pandit, Central Department of Physics, IOST, Tribhuvan University, Kirtipur, Kathmandu, Nepal. (drabindrapandit087@gmail.com)